RESEARCH
O&G Forum 2024; 34-3s: 2787-2799

HISTOGRAM BASED TUMOUR CLASSIFICATION FOR BRAIN MRI IMAGES USING ANN

N SATHISHA

Assistant Professor, Department of ECE, Govt. S K S J Technological Institute K R Circle Bangalore 560001, India, nsathisha@gmail.com

Abstract

This paper presents a novel approach for the classification of brain tumours in MRI images using histogram-based features and Artificial Neural Networks (ANN). Accurate classification of brain tumours is crucial for effective diagnosis and treatment planning. Traditional methods often rely on complex pre-processing and feature extraction techniques, which can be time-consuming and computationally intensive. Our methodology simplifies this process by leveraging histogram features that capture the intensity distribution of pixels within the tumor region, providing a straightforward yet powerful representation of the image data. The proposed system involves several key steps: pre-processing the MRI images to enhance quality and consistency, extracting histogram features from these images, and then using these features to train an ANN model. The ANN, designed with multiple hidden layers, is optimized to distinguish between benign and malignant tumours based on the input histogram data.

our system is evaluated using a comprehensive dataset of labelled MRI images, and the results demonstrate its high accuracy and reliability. The classification accuracy achieved was [insert accuracy percentage here], indicating the robustness of our approach. The use of histogram features not only simplifies the feature extraction process but also enhances the ANN's performance by providing relevant and discriminative information about the tumor characteristics. This study highlights the efficacy of combining histogram-based feature extraction with ANN for brain tumour classification, offering a viable solution that improves diagnostic accuracy and efficiency. The findings suggest that our method can significantly aid in the early detection and accurate classification of brain tumours, potentially leading to better patient outcomes and optimized treatment strategies. The simplicity and effectiveness of this approach pave the way for further advancements in medical image processing and diagnostic techniques.

Keywords: Artificial Neural Network (ANN), Benign Tumor,, Brain Tumor Classification, Diagnostic Accuracy, Feature Extraction, Histogram Features, Image Preprocessing, Magnetic Resonance Imaging (MRI), Malignant Tumors, Medical Image Processing.

I. Introduction

The field of medical image processing is critical to contemporary healthcare, using computational techniques to improve the collection, examination, and interpretation of medical pictures. The identification and treatment of brain tumors, one of the most difficult and potentially fatal diseases, is one of its most important uses. Brain tumor diagnosis, characterisation, and treatment planning are greatly enhanced by medical image processing using cutting-edge imaging modalities, especially Magnetic Resonance Imaging (MRI).

Strong magnetic fields and radio waves are used in magnetic resonance imaging (MRI), a non-invasive imaging method, to provide detailed images of the brain. Because of its better contrast resolution, which enables the precise viewing of soft tissues, it is very useful in the diagnosis of brain tumors. MRI can distinguish malignancies from healthy brain tissue.

Uncontrolled cell proliferation, a breakdown in the regular rhythm of cell death, or both may lead to tumor formation [1]. There are two types of brain tumors: primary and secondary. Primary tumors are made up of cells that originate from the same organ or tissue as the tumor. Any area of the brain can be affected by a tumor, and depending on which area of the brain is affected, there can be a variety of symptoms, such as mood swings, seizures, and problems with language, vision, hearing, sensation, and muscle movement. Gliomas, Medulloblastomas, Ependymomas, CNS Lymphoma, and Oligodendrogliomas are the different types of brain tumors. Gliomas represent 70% of adult malignant primary brain tumors and are the most common primary brain tumor in adults [2].

Brain tumors typically do not contain cancerous cells, can be surgically removed, and rarely recur. One may easily detect the edge or boundary of an initial brain tumor. Human inspection is the standard method used in medicine for classifying brain MR images and detecting tumors. Large data sets make operator-assisted categorization techniques unfeasible and non-reproducible. The World Health Organization (WHO) created the most widely utilized grading scheme in use today [3–4].

The location and rapid spread of brain tumors pose significant challenges to tumor treatment. As a result, image segmentation and detection are dynamic approaches to treating a wide range of medical conditions [5–6]. There are several methods for imaging brain tumors, including ultrasound, magnetic resonance imaging (MRI), and computed tomography (CT) scans. In this paper, the system is implemented using an MRI scan. In order to identify and detect brain cancers more effectively, a number of approaches have been developed. Fuzzy C Means Algorithm [10], neural network algorithm [8], watershed and edge detection [9], modified texture-based region growth and cellular automata edge detection [7], and so on are a few examples. Brain asymmetry is utilized to identify abnormalities [11]. Significant grey level asymmetries are produced by tumors in brain MR images [12]. Grey level

symmetry analysis can be used to identify tumor presence. Because of its many significant applications, edge detection is one of the most appealing challenges to the image processing community. In order to handle the correct feature extraction, cranny edge detection is frequently employed to generate features for image segmentation [13–15]. The F-transform [16–17] is a clever and effective way to deal with ambiguous data. It is a representation of the natural occurrences we actually witness in our daily lives. The F-transform methodology is a promising and effective way to extract features and edges, as demonstrated by DaĖková and Valášek [18].
In order to solve the accuracy and computational issues, we create an algorithm in this study for the detection and segmentation of brain tumors. For the suggested algorithm, there are two primary phases that are completed. The initial phase is predicated on the investigation of brain asymmetry. Since the midsagittal plane of a healthy human brain is typically symmetrical bilaterally, symmetry analysis of grey levels is used to identify tumor presence. Segmentation based on edge detection is the second step. We provide a novel approach to edge identification that utilizes the F-transform model to identify quiet edges [6]. Following edge extraction, morphological operations were used to show only the tumor in the final stage. MRI data of brain tumor images [23] from several patients have been used to test the method. The algorithm's accuracy and efficiency are shown by the experimental results.

II. Summary of Literature survey.

Brain tumor analysis, surgical planning, and measuring and visualizing the anatomical structures of the brain are all made possible by the segmentation of brain MR images. Similar research yielded results that showed how different approaches and methodologies might be combined to segment and detect tumors in 2D brain MR images. On the other hand, the exact results were not demonstrated in the relevant study works for the 3D brain MR image segmentation and tumor detection. Therefore, the goal of this suggested work was to design an automatic integrated segmentation framework that used both the Fuzzy C Means [6-7] Clustering approach and the most well-known enhanced EM (Expectation Maximization) method for the detection of tumors in brain 3D MR images. The suggested framework shows an improvement in the segmentation of brain MR images by appropriately combining the segmentation findings of the most well-established method. To increase the quality of the brain MR image and to create better tumor segmentation and identification, the most widely used anisotropic filter is used to the improved EM (Expectation Maximization), Fuzzy C Means Clustering Method, and Proposed Augmentation Method. Real brain datasets and simulated brain Fluid-Attenuated Inversion Recovery MRI images are used to assess the performance outcomes using CNN [21]. The segmentation accuracy, sensitivity, and specificity of the suggested work are quantified, and the performance results outperform those of the state-of-the-art approaches.
Brain tumors are a major cause of morbidity and death globally, and improving patient outcomes requires early detection and accurate diagnosis. Magnetic resonance imaging (MRI) is the most common method used to find brain tumors, albeit it can be challenging to accurately diagnose tumors from images. In this paper, we propose a deep learning method based on MRI data for brain tumor diagnosis. In order to accurately identify and categorize brain tumors, our approach uses a Deep Convolutional Neural Network (DCNN) architecture [17]. Gradient-weighted class activation mapping, or Grad-CAM, is utilized to visualize data in the brain tumor area. Our goal is to help cancer patients and/or medical staff with patient diagnostics. We examine our approach, which yielded a high degree of accuracy (97%) together with excellent precision, using a dataset from Kaggle that included 2114 brain MRI pictures. Our findings demonstrate the effectiveness of our suggested approach for diagnosing brain tumors, and the application of Grad-CAM [20] allows us to view the brain regions most closely associated with tumor identification, offering physicians important new knowledge. Furthermore, our findings can be applied to the identification of infectious diseases by appropriately modifying the parameters.
In order to detect and calculate the volume of brain tumors, this study examines two-dimensional magnetic resonance imaging (MRI) sequences of brain slices that contain a variety of objects. In order to detect and characterize the tumor, more than twenty-five features based on shape, color, and texture were extracted, and feature vectors were created for each object. The outcomes of the experiment demonstrate how accurate the tissue volume estimation is. The most severe kind of tumors are brain tumors, which are caused by the proliferation of cells inside or outside the brain. Brain tumors are defined as any abnormal mass of cells within or around the brain that has the potential to become malignant. Our suggested method uses MRI scans from MRI images to locate and identify the brain tumor. CNNs and deep learning techniques are used in this study to detect brain tumors [19]. When these algorithms are applied to the images, brain cancer cells can be detected more quickly, correctly, and effectively, leading to the provision of better and more advanced treatment for the patient. BTC helps health monitors and radiologists provide patients with timely medical attention. We will obtain greater accuracy with our methods.
The diagnosis of brain cancers with magnetic resonance imaging (MRI) is a critical challenge in medical imaging that is sometimes complicated by noise and imaging process flaws. In this work, we provide a unique methodology that combines convolutional neural networks with sophisticated denoising and classification techniques to improve the precision and dependability of brain tumor diagnosis using MRI data. In the denoising step, important picture attributes are preserved while noise is effectively removed using the OpenCV library's cv2.fastNlMeansDenoising algorithm [20]. The VGG16 classification model, which is renowned for doing remarkably well in image recognition tasks, is then fed the preprocessed images. Our approach makes use of the spatial correlations shown and the discriminative abilities of VGG16 in an effort to achieve higher classification accuracy than traditional techniques. The effectiveness of the suggested method is demonstrated by experimental findings on benchmark MRI brain tumor datasets, which show significant gains in tumor identification accuracy and robustness against noise. This innovative method may enhance clinical processes and patient outcomes with neuroimaging diagnostics.

III. Proposed Methodology
SEGMENTATION OF BRAIN MRI IMAGE

Segmentation of image is the processing of image to extract only the desired area in the image. Performing segmentation for an image depends on number of parameters like texture, colour, brightness, etc. An optimization is defined as recognizing and partitioning of desired surface parts in an image and the regions with respect to structural features.

A. Image Segmentation Methods

1. Segmentation of image based on Threshold: In this method of segmentation, intensity of the pixels is considered as a parameter. Either global threshold or local threshold are used as cutoff value to make decision. The global threshold partitions the desired area of image by applying binary rule. Regional or local threshold methods are used for applications where dynamic adaptiveness is needed. The value of the threshold is based on the local features of the area of the image to be partitioned or identified. Histogram techniques, pre-processing methods, techniques of sub-processing are used in this type of segmentation. The popular threshold based segmentation techniques are p-tile method, mean value method, based on histogram technique, maximizing edge method, visual methods and other.

2. Segmentation of image based on Similar Regions: All the pixels that belong to the one object or similar object are classified by using this type of segmentation. The object area has to be locked so that optimization can be obtained in the segmentation. The segmentation borders are identified by the edge pixels. The variation in the area or the region can be identified by using texture, colour or the stem-flow, which was generated as a vector. This also explains the need for the further maximizing [7].

3. Segmentation of image based on Edges: This method of segmentation partitions the image based on the intensity of pixels. The edges will be detected by measuring the pixel amplitude or the difference in the pixel's amplitudes for the considered frame size. An important phase in the image segmentation is identifying the blade [18]. This partitions the given image and gives its significance as entity. Major methods for performing identification of blade for color differentiation are gradient method and gray-histogram method. In few methods, detection of the edge is also done and the methods are classical boundary detecting method, zero-crossings method, LoG – Laplacian method, Guassian Laplace method, sensors for light edges, etc.

4. Segmentation of image based on Fuzzy Theory: In order to obtain trustworthy data from each image for the purpose of image interpretation, fuzzy set theory is utilized. Image noise can also be reduced by using fuzzification [4]. A fuzzing feature makes it simple to transform a grayscale image into a fluid one. A fugitive strategy may combine many morphological processes for improved outcomes [5]. In image processing, fuzzy K-means and fuzzy C-means are frequently used techniques.

5. Segmentation of image using ANN: In order to provide accurate information from each image for image interpretation, fuzzy set theory is utilized. To lessen picture noise, the fluxing technique can also be used [3, 6]. It is simple to transform a grayscale image into a floating image. Such fluffy strategy can be used with various morphological actions to get superior results [6]. C-means and image processing are frequently employed.

6. Segmentation of image based on PDE: PDE - Partial Differential Equations formulas or models are frequently utilized for image analysis and for optimizing. Their segmentation method is based on active contour pattern. The contour system, often known as snakes, is a successful method of converting optimization problems into PDEs. Several popular PDE techniques for photo optimization are the Mumford Shah System, Level-Set, and Snakes methods[4, 6]. This section discusses a few novel methods for PDE picture segmentation. [8].

IV. DETECTION OF BRAIN TUMOR

The human central nervous system has always been centered on the brain. There are between 50 and 100 billion neurons in this vast network. The brain is an intricate organ. An aberrant collection of brain-borne or cross-brain cells is referred to as a brain tumor. There are two types of brain tumors: benign and malignant. Benign Tumors are the non-cancerous tumors. In order to effectively treat the surrounding imaging patches for tumor-infected human brain MRI, this paper look at recent advances in image segmentation and classification. These patches can move across the network with a glioma goal while also being adjusted to robot imbalances in 3D scans. Malignant tumors are those that have been distinguished from primary and secondary tumors [9]. The cancerous growth swiftly invades other.

For certain patients, a proper diagnosis of a brain tumor might mean the difference between life and death. The most popular method for detecting brain tumors is MRI. Treatment for brain tumors consists of basically four core steps:

1. Initial processing: Pre-processing produces a sharper image of raw MRI scan. It suggests that accurate and precise optimization is directly related to preprocessing. Pre-processing operations include image improvement, skull scraping, and de-noise[1].

2. The Extraction of Features: This method yields a collection of traits that interpret a picture. In particular, it is the essential task for the segmentation of brain tumors [3].

3. Segmentation: The cycle of enhancing aberrant brain tissue, such as cells, the necrotic heart, and edema, differs from normal brain tissue. The three primary categories of brain tumor activity were determined using segmentation processes that were manual, semiautomated, and fully automated. There are numerous approaches for tumor segmentation, such as machine learning, asymmetry, regional, intensity, and machine learning methods[6].

4. Post Processing: For better outcomes, these post-processing techniques include spatial control, shape limitations, and contextual constraints. This method offers a clear visual representation of the tumor area's brain anatomy. Additionally, brain tumor research and treatment are conducted using the image[10]. Compared to benign tumors, the malignant form grows more quickly. The healthy brain cells are also impacted by such a tumor. The tumor may recur even after surgery. It could spread to the backbone or other parts of the brain. Secondary brain tumors develop in other parts of the body, such as the kidneys, breast, and so forth, and then spread to the brain.

Different methods, like MRI and CT scans, can be used to scan the brain in different ways, at different levels, and both horizontally and vertically. For this, we used an MRI picture from the horizontal portions. There are three forms of growing tumors:

- **Benign Tumor:** A brain tumor that is benign (non-cancerous) is a mass of cells that is slowly growing within the brain. Normally, it remains in one location rather than dispersing. The location and size of the brain determine the symptoms of a benign brain tumor. Slow-growing tumors might not show symptoms right away. Severe headaches, convulsions, frequent nausea, vomiting, and sleeplessness are frequently experienced.
- **Pre-Malignant Tumor:** Precancers, also known as premalignant diseases, are often referred to as precancerous disorders or potentially premalignant diseases. Precancers are states of unstable cell morphologies linked to an elevated risk of cancer.
- **Malignant tumor:** Cancerous tumors are malignant tumors, which have a slow-growing appearance and can be fatal. Malignant tumors grow more quickly, are more aggressive, search for new areas to spread, and metastasis than healthy ones. A malignant tumor's abnormal cells spread more quickly [22].

V. MAGNETIC RESONANCE IMAGING

In medical imaging techniques, magnetic resonance imaging (MRI) can offer comprehensive information on the internal structure of corresponding images. Determining the precise location of the tumor is crucial for treating brain tumors since it helps determine the tumor's size and kind. Brain tumor detection technology relies heavily on imaging segmentation; many imaging modalities are processed from brain magnetic resonance images to identify tumors. Segmented information about soft brain tissue, including CSF (cerebral spinal fluid), white matter (WM), and gray matter (GM). Manual and automatic segmentation are the two types of segmentation. Although manual segmentation technology is labor-intensive and dependent on human expertise, it reduces computing efficiency. On the other hand, automatic segmentation revolves around the histogram. The only basis for this is pixel pressure. The existing methods for identifying or segmenting brain tumors from MRI images have been incorporated into this study (e.g. threshold-based, edge-based, geographic or clustering segmentation). The following goals for the automatic detection and segmentation of brain tumors from MRI images are depicted in Figure 1, and Figure 2 shows the matching suggested system.

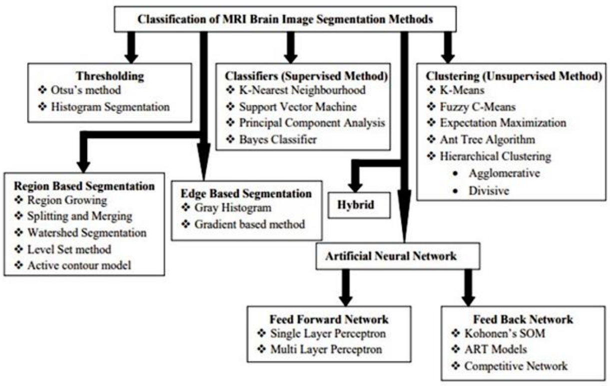

Figure 1: Classification of MRI brain images.

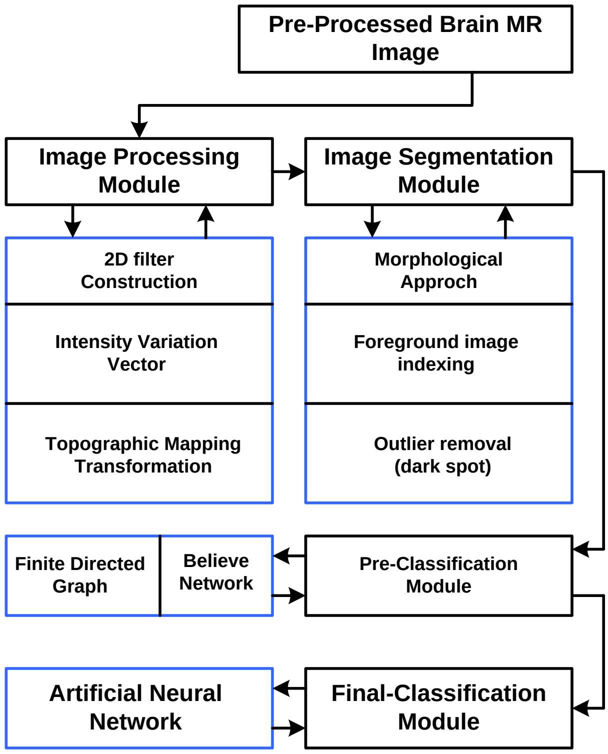

Figure 2. Block diagram of the proposed system.

MRI Image Segmentation for Brain Tumor

This section discusses the image segmentation processes adopted in the proposed framework, which is explicitly different from the other existing segmentation mechanism. The proposed framework utilizes multiple mechanisms that boost the segmentation process to obtain superior classification operation quality. Therefore, the system implements a morphological approach to recognize and localize the size of a brain tumor. This operation uses a structuring element, the construction of a small two-dimension matrix of morphological structure. Such elements are applied here to interact with the input image to produce a resultant foreground image. The structuring element is constructed with a disk-like shape with a radius value equal to enhancing the morphological operation's dilation and erosion process. The radius of the structuring element function as a ‘window' over which the interaction takes place and the shape of such element is a representation of zeros and one's element within the 2D matrix, where one represents neighboring elements of binary value which used to discarding false pixel elements and considering only true pixel. Thus, the reference pixel located at the center is considered to perform recognition of true and false pixels. This type of segmentation operation is applicable for both binary image and grayscale MR brain images. This process produces a mapped version of the input brain MRI and a morphological eroded image. The obtained erosion image is further subjected to reconstruction operation. Therefore, this operation generates a foreground indexed image. A similar operation is then carried by applying the morphological dilation process on the reconstructed image considering the structural elements. Again reconstruction process is now performed on the obtained dilated image, and then the complement image of the recently obtained expanded image is calculated. As a result of this operation, the brain MRI image's darker areas become lighter areas, whereas the lighter areas become a darker area. Finally, the largest area/region is achieved to aid the segmentation operation. The next section describes the computing procedures involved in the implementation of the above-discussed operations.

Computing Steps for Image Segmentation Process

Step-1. Initialize S_E, $ɱ_1$, $ɱ_2$, $ɱ_3$, $ɱ_4$
Step-2. Load $\rightarrow I_m$
Step-3. Compute S_E (Structural element)
- a. $S_E \rightarrow f_m(s, r)$

Step-4. Perform Image Opening
- a. $ɱ_1 \rightarrow f_{m1}(I_m, S_E)$

Step-5. Compute eroded image
- a. $ɱ_2 \rightarrow f_{m2}(I_m, S_E)$

Step-6. Perform reconstruction
- a. $ɱ_3 \rightarrow f_r(ɱ_2, I_m)$

Step-7. Display $\leftarrow ɱ_3$-(Foreground indexing image)
Step-8. Perform image closing
- a. $ɱ_4 \rightarrow f_{m3}(ɱ_1, S_E)$

Step-9. Display $\leftarrow ɱ_4$-(outlier eliminated)
Step-10. Perform image Dilation
- a. $ɱ_5 \rightarrow f_{m4}(ɱ_3, S_E)$
- b. compute complement of image
  - i. $ɱ_6 \rightarrow f_c(ɱ_5, ɱ_3)$
  - ii. $ɱ_7 \rightarrow f_r(ɱ_6)$
  - iii. $ɱ_7 \rightarrow f_c(ɱ_7)$

Step-11. Compute regional maxima and superimpose
- a. $g_{mx} \rightarrow f_g(ɱ_7)$
- b. $I_{super1}(g_{mx})=255$, where $I_{super1,2} \leftarrow I_m$

Step-12. Edge cleaning
- a. $I_{super2}(f_{m5}(f_{m2}\ (f_{m3}(g_{mx,}(f_m([1]_{5\ x\ 5}),\ f_m([1]_{5\ x\ 5}),\ P))=255$

Step-13. Display Image $\leftarrow I_{super2}$(Segmented image)

Illustrations

The above-presented computing steps implemented for the image segmentation process, which initially assigns variables such as S_E-(Structural element), $ɱ_1$, $ɱ_2$, $ɱ_3$, $ɱ_4$ (the computed result of various morphological operations) (Step-1). This module's next process is to load input brain MR image (I_m), which provides an outcome of segmented brain image after executing further morphological and image indexing processes. After successful loading of I_m, the system constructs structuring element-(S_E) using morphological function f_m with considering characteristics S (shape), r (radius), and a (disk approximation). The system assigns structuring element shape like disk and the size in terms of radius equal to positive-integer value 10. The construction of disk S_E is computed in small 2D matrices, which are further used to interact with the I_m (Step-3). The system considers the center's reference pixels to identify true pixel values and false pixel values. However, it is not restricted to consider reference pixels at the center. However, it is a convenient way to identify valid pixels because the S_E patterns with the values of zeros and ones where the values 'ones' define the adjacent pixels and the zeros are not considered a non-active member.

The basic objective behind S_E's interaction with I_m is to perform the transformation of S_E's reference pixel to the entire pixel of the I_m, and the outcome is achieved by using further morphological operations. After constructing S_E, the system performs its next operation of computing the image's opening ($ɱ_1$) using morphological function f_{m1} over the computed S_E and the I_m (Step-4). The function f_{m1} refers to the joint procedure of erosion and dilation. The $ɱ_1$ of I_m followed by S_E is represented in the numerical equation (1) as follows:

$$ɱ_1 = (I_m \ominus S_E) \oplus S_E \ldots \text{(eq.1)}$$

The above mentioned numerical equation (1) illustrates the computation of $ɱ_1$ by the erosion of an I_m by a S_E, and the resultant is dilated with the same S_E. Figure 3 shows the opening of image by the done by the structural element S_E. The opening operation performs the outline smoothing operation of an object and eliminates minor extensions and gaps.

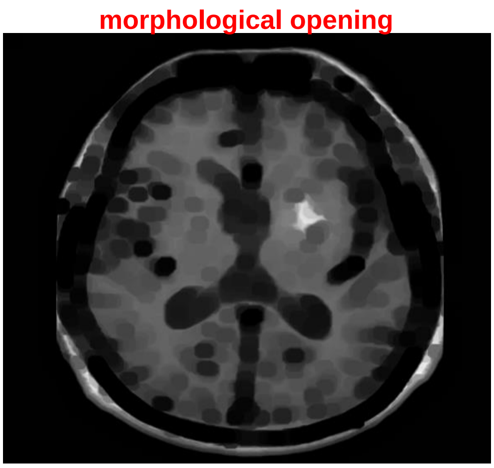

Figure 3 Opening of image

The system's next process is to acquire an eroded image ($ɱ_2$) using another function f_{m2} over I_m and S_E (Step-5). The function refers to the process of erosion operation. Therefore, the computation of $ɱ_2$ is achieved by the erosion operation, as demonstrated in equation (2) as follows:

$$ɱ_2 = \{k \mid (S_E)_k \subseteq I_m\} \ldots \text{(eq.2)}$$

Where k is a position of pixels and $ɱ_2 \rightarrow I_m \ominus S_E$

The above highlighted numerical expression (5.2) demonstrates the computation of $ɱ_2$ considering I_m, and S_E set of all points k such that the structuring element S_E is transformed by k is a subset of the Im.

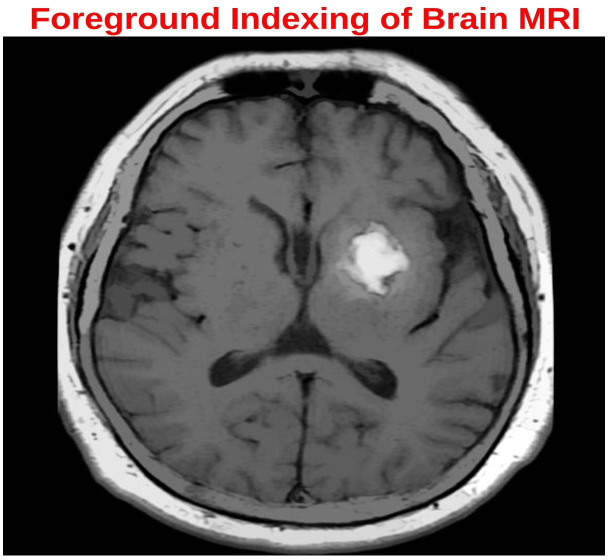

Figure 4 Foreground indexing of input image

This process highlights pixel (zero) the background of an object and narrows down the object's foreground's pixel value (one). This operation eliminates unwanted pixels containing the smaller size of structure than the S_E and provides resultant values (ɱ_2) as an enhanced sharpness of the image's object. However, ɱ_2 is not the final eroded image. Therefore the system performs reconstruction of ɱ_2 using function f_r *(Step-6)* over the I_m, and $\text{ɱ}_2$which provides a final output (ɱ_3) as foreground indexing as shown in Figure 4 (Step-7).

After obtaining a value of ɱ_3, the next process is to perform a closing morphological operation on the ɱ_1 with S_E using function f_{m3} (Step-8) to eliminate the outlier spots from ɱ_1. This function refers to a similar joint operation of erosion and dilation. However, both the opening and closing of an image are different operations, which can be seen from equation (1) and equation (2). Hence the computation of closing of image (ɱ_4) is obtained as follows:

$$\text{ɱ}_4 = (\text{ɱ}_1 \oplus S_E) \ominus S_E \ldots \text{(eq.3)}$$

The above numerical expression (3) states the closing operation using both erosion and dilation operation where the opening image (ɱ_1) is dilated by S_E, and its resulting value is eroded by the S_E. Therefore, the closing of image (ɱ_1) is represented in Figure 5 as follows (Step-9):

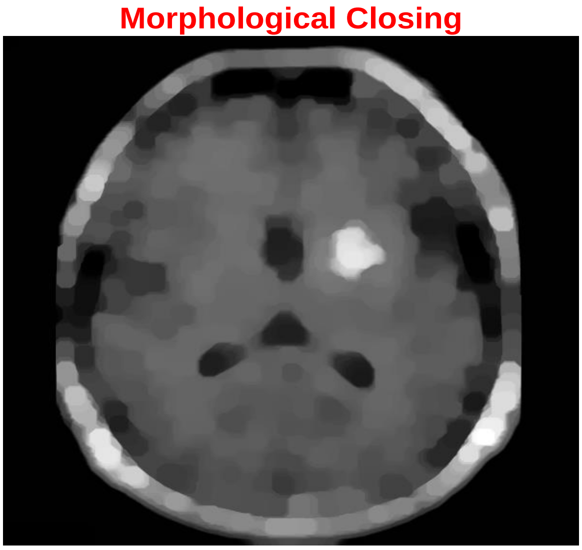

Figure 5 Blackspot and outliers eliminated

The above Figure 6 exhibits the closing operation on image to obtain the clean and sharp object image structure, which combines narrow fractures and small gaps, eliminates small holes and fills the gap in objects' boundaries.

The next process (Step-10) is to use function $f_{m4}$to compute dilated image (ɱ_5), which results in the extended size of the object in an image. However, the size extension operation is highly dependent on the nature and characteristics of S_E. The computation of ɱ_5 is obtained by using morphological dilation operation using numerical expression (4) as follows:

$$\text{ɱ}_5 = \{k \mid (S_E)_k \cap \text{ɱ}_3\} \ldots (4)$$

Where k is a position of pixels and $\text{ɱ}_5 \rightarrow \text{ɱ}_3 \oplus S_E$

Therefore, the dilation operation on the image (ɱ_3), which is computed in the above Step-6, provides us an expended size of an image's object with smoothed structure. The next step is to carry a complement of the image, which converts image area such as black area transforms into white and white area transform into black. The system uses a function $f_c(x)$ over ɱ_5 and ɱ_3 for attaining the image compliment (ɱ_6) concerning reconstruction image (ɱ_7) using $f_r(x)$ function over ɱ_6. The next process further computes the complement of image (ɱ_7) using function f_c applied over it (Step-10 b). Further, the system performs its next operation to compute the recently computed image's regional maxima-(ɱ_7). For this, a new variable is assigned as g_{mx}, which uses a function f_g over ɱ_7, which detects the position of regional maxima in the ɱ_7 using the connected component of image pixels. After this, the regional maxima (g_{mx}) are superimposed into the input image (I_m) (Step-11). The next computing step carries operation to clean edges of the superimposed image obtained from the computation of Step 11(b). For this, the system use function f_m to constructs another structuring element-(S_{E2}) of a matrix having a dimension of 5 x 5 and then performs a morphological closing operation using function f_{m3} over g_{mx} with S_{E2}, which is further eroded by applying function f_{m2}. After computing this new version of an eroded image, the system then applies another function f_{m5}, to perform an area opening operation where a small connected component is eliminated with less size than the pixel size of an image. The newly obtained image is then gone for the superimposition process on the input image (I_m), giving the final value of a segmented image in the form of edge cleared image.

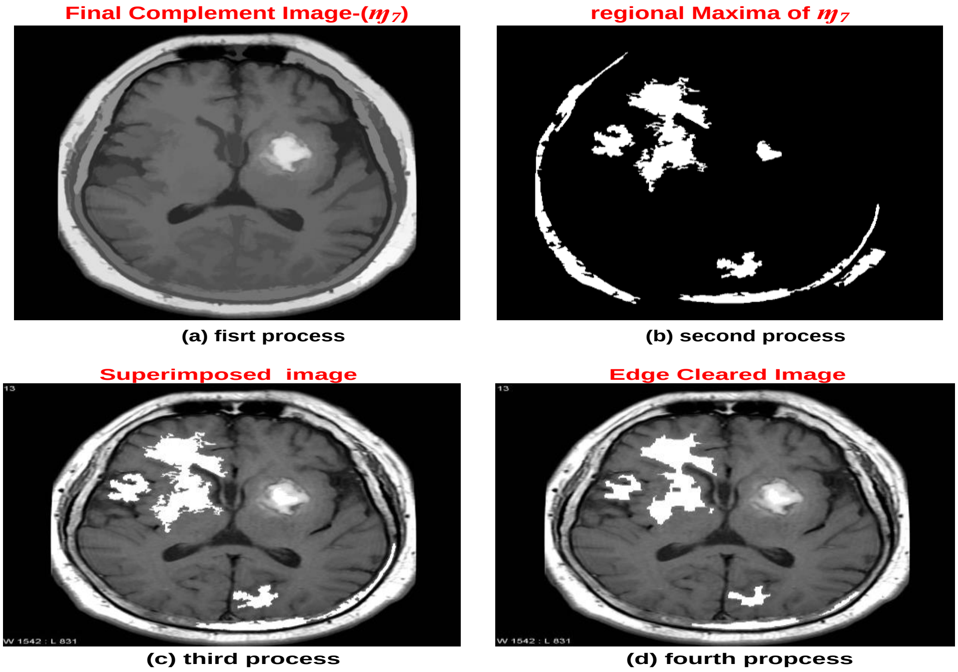

Figure 6 Initial image segmentation processes

The Figure 6 demonstrates the computed result of ŋ$_7$ (final complement of image), which is the initial computed image towards segmentation, g_{mx} (regional maxima) as a second process that is then superimposed with the input and edge cleared image as a final segmented image. The discussion of current procedures presents a series of image processing operations to obtain an initial segmented image observed in the above processes as computed and demonstrated in pictorial representation. Therefore, the segmentation process is followed by various image analyses and filtration operations, which act as complimentary services towards performing better abnormalities classification from the input brain MRI image. The next section presents its next contribution to initiate the execution of the pre-classification module.

Initiating pre Classification Process

This section describes the pre-classification module, which consists of several computing procedures and techniques. Here, initially, the compliment image obtained in the previous section is subjected to the binarization process concerning its grayscale thresholding. The acquired binary matrix now goes through the computation process to calculate the Euclidean distance among the obtained binary images' elements. Furthermore, the initial segmentation operation using the topographic concept is then performed on the binary image to compute a more segmented version of the image. Thus this process helps to perform indexing the background of the image. The intensity factor for a better classification process is also required to be controlled in the final process. This operation changes the image's intensity utilizing the reconstruction process of the morphological, structural elements in respect of I_{vv}, the concatenation of the indexed background, and the complementary image. The obtained image is then processed with topographic representation, which offers better segmentation processes, thus generating enhanced classification results. Afterward, the system applies the concept of graph theory, which mainly concentrates on the edges and vertices for better classification assistance instead of forming various loops. After this process, a belief network is constructed, which provides advantageous features to compute the decision-making process even in the presence of dynamic and varied sequences. Another advantage is that it can efficiently handle all kinds of missing values and make better predictions using statistical values. The process then performs the region merging operation by obtaining the all-region matching to the belief network and then applying a histogram on it.

Computing Steps for initiating Classification process

Step-1. Load ŋ$_7$
Step-2. Perform binary conversion operation
  a. $I_b \rightarrow f_b(ŋ_{7,}\ \tau_g)$
Step-3. Compute Distance Transformation
  a. $\mathcal{E}_d \rightarrow f_d\ (I_b)$
Step-4. Compute watershed region
  a. $I_{b2} \rightarrow g_1(\mathcal{E}_d)$
Step-5. Compute background indexing
  a. $I_{bindex} \rightarrow (I_{b2} == 0)$
Step-6. *Display* I_{bindex}
Step-7. Compute Segmentation using T_R *Concept*
  a. $I_{vv2} \rightarrow g_m(Ivv,\ I_{bindex}|I_{super2}\ ))$
  b. $\beta_{i2} \rightarrow g_1(I_{vv2})$
Step-8. Visualize Segmented Image
  a. $\beta \leftarrow g_2(\beta_{i2}\ )$
Step-9. Display β
Step-10. Construct a Directed Graph
  a. *Initialize Link Map*
    i. $L_M \rightarrow O_{(fmax(\beta i2))} = [\ ]_{m\ x\ n}$

b. *Assign label to all region*
   i. *For* $i_l = f_{max}(\beta_{i2})$
c. *Compute region-(R) and its adjacent regions*
   i. $R \leftarrow i_l$
   ii. $R_{adj} \leftarrow f_m(f_{m4}\ (R,, 2))$
d. *Compute Labels(L) and extract non-repetitive value*
e. *Assign respective link value to 1 and compute coordinates corresponding to R*

Step-12.Construct Belief Network(B_{Net}*)*
a. *Create cell array* $\leftarrow f_{names}[]_{1\ x\ (fmax(\beta i2)}$
b. *Compute total coordinates points (P)* $\leftarrow f_{max}(\beta_{i2})$
c. $B_{Net} \rightarrow f_{Bnet}(L_{M,}\ 2,\ cell\ array\ )$

Step-13. Display B_{Net}

Illustrations

The first step towards initiating the classification process starts with taking input values of ŋ$_7$ (segmented region), which provides its outcome as a classified segmented region (C) (Step-1). The system initiates computing operation for the binary conversion process to acquire binarized image I_b by applying a function $f_b(x)$ over ŋ$_7$ (i.e., morphological elements which are computed in the above segmentation process) and τ_g (gray thresholded image of ŋ$_7$) (Step-2). The gray thresholded image is computed using Otsu's method, which uses a threshold factor to convert the intensity image into a binarized version. The next step is to compute distance transformation in the binary image (I_b) using function f_d, which refers to a Euclidean distance formula to compute spatial space of length between the elements in I_b. The computation of spatial space of length using a Euclidean distance formula is illustrated in equation (5).

$$\frac{\mathcal{E}_d(I_b)=|a-b|}{\sqrt{(a1-b1)^2+(a2-b2)^2+\cdots+(a_n-b_n)^2}} = \sum_{i=1}^{n}(a_i - b_i)^2 \quad \ldots \text{(eq.5)}$$

The next step is to compute the watershed region using function g_1 *over* $\mathcal{E}_d$ for topographic mapping transformation to obtain background indexing (I_{bindex}) (Step4 and Step5). Figure 7 demonstrates the indexing of the background image as follows:

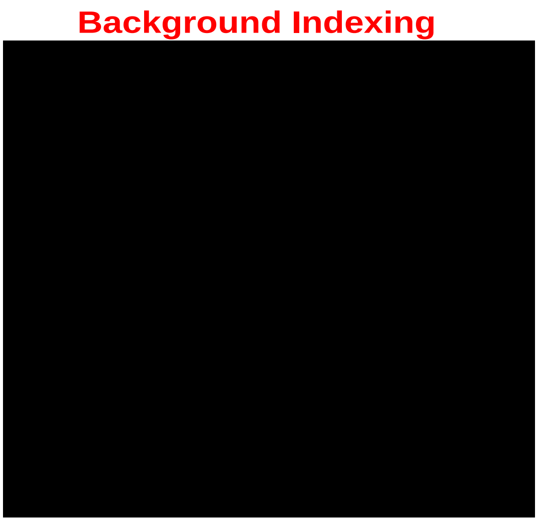

Figure 7. Indexing of back ground

The next step is performing a computing procedure for segmentation using values obtained from I_{bindex}, I_{vv}, $I_{super2,}$ followed by a topographic representation process. Therefore, the system assigns a new variable I_{vv2} and where minima of the image are extracted considering I_{vv} values and concatenation of recently obtained I_{bindex} and $I_{super2,}$ computed in the previous segmentation computing process (Step7). The second stage creates the second version of the segmented image (βi2) by performing a watershed transformation over the Ivv2 using a similar function g1. The format is then obtained by applying function g2 over βi2 to see the final output (β2) of the segmented image in color. An additional version of the segmented image (β2) is produced by this process. The colored segmented images in Figure 8 is shown.

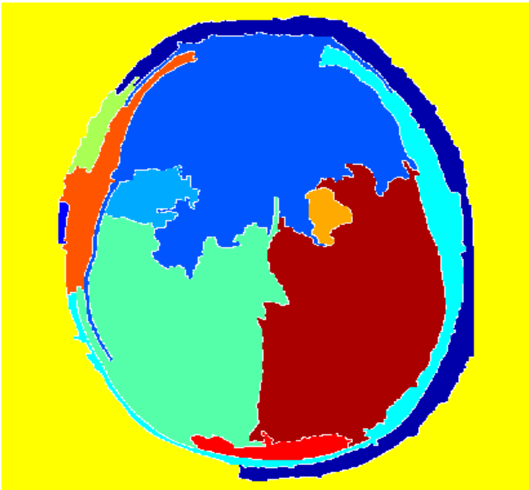

Figure 8 Colored segmented image (β_2)

After computing the new segmented image, the next process is the construct directed graph. For this, the system first initializes connection or link map by creating a zero matrix of the size of the largest element in β_{i2} to store values associated with the finite graph. The next process is assigning labels at all regions β_{i2}. Thus, the system computes the region and its adjacent regions. The region's value is equal to the largest element of the $\beta_{i2.}$ The adjacent region's value is extracted using a morphological function with dilation operation on region R with N number of iterations in which dilation operation is performed until the region R no longer changes. After getting region and adjacent regions, the system computes non-repetitive values, further subjected to connection and coordinate computation corresponding to region R (Step-10). This provides a finite directed graph, and therefore, the next process constructs a belief network using a cell array of size one x largest element of $\beta_{i2.}$ The next process is the computation of absolute coordinates points from the $\beta_{i2.}$ Afterward, the construction of the belief network is executed using Bayesian network function f_{Bnet} over the link map (Lm) constructed in the above procedure of directed graph, coordinate point size (i.e., 2), and cell array f_{belief}. This operation provides adequate accuracy in the classification process. Figure 9 demonstrates the out of the above operations. This step is a continuation of the above operations, which computes the region histogram of β_{i2} to obtain primary classified image C.

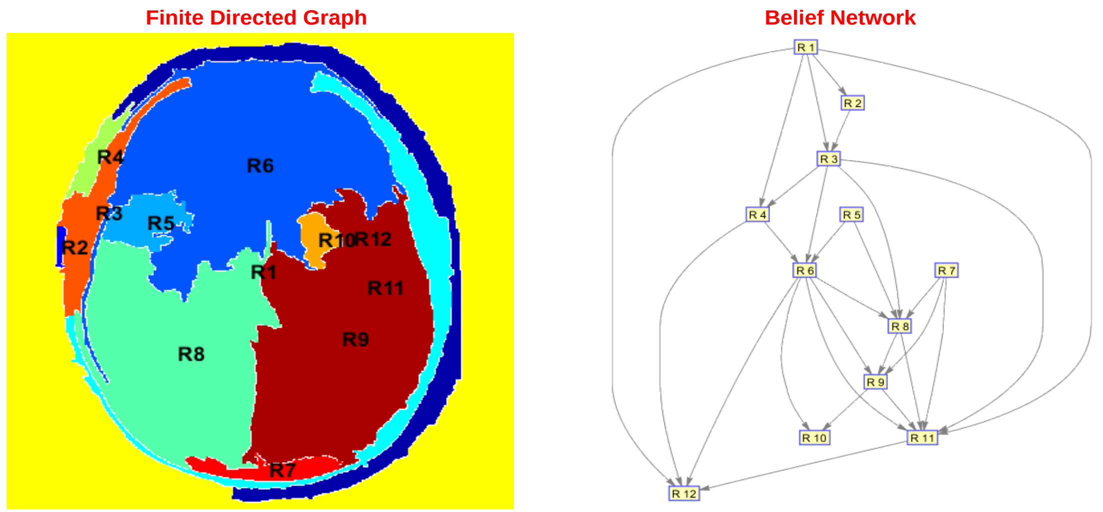

(a) (b)

Figure 9 Directed graph and belief network

Computing Steps for Region histogram and histogram merging

Step-1. Create cell array ← $f_{hist}[]_{m\,x\,n}$

Step-2. Compute Histogram for each region

a. For i = 1:fmax(β_{i2})

b. Get region: R ← $\beta_{i2} == i$

c. *Get R pixel value(R_{pv})* → $I_m(R)$

d. *Hist* ← $f_h(R_{pv}, 255)$

e. *Store Hist* → $f_{hist}[]_{m\,x\,n}$

f. *End*

Step-3. Display C (primary classified image)

Step-4. Perform Region merging

Step5. Construct a zero matrix of size L_M

a. cpt ← $O_{LM} = [\ ]_{m\,x\,n}$

Step-6. Compute the number of overlapping factor between two statistical sample

a. *For i =1:* $f_{max}(\beta_{i2})$

b. *Extract connected component for each segment*

i. CC $= f_e(L_{M,}\ (i_l))$

c. *Get histogram of current point P and connected point P1*

d. *Ovf* → $f_s(\sqrt{P * P1})$

e. *End*

f. Store this in cpt → *Ovf/*($f_s(P+P1)$)

Step-7. C ← $f_l(B_{Net,}$cpt, $\beta_{i2})$

Illustrations

The system constructs an empty cell array to computing the region histogram (Step-1). The next process is to carry a histogram for each region of β_{i2}. For this, a region pixel values are carried out from the input image (I_m), which is further subjected to the computation of histogram for each region using function f_h over region pixel value-(R_{pv}) and color map (Step-2). The computed value of the histogram is shown in Figure 10 which is stored in the cell $f_{hist}[]_{m\,x\,n}$.

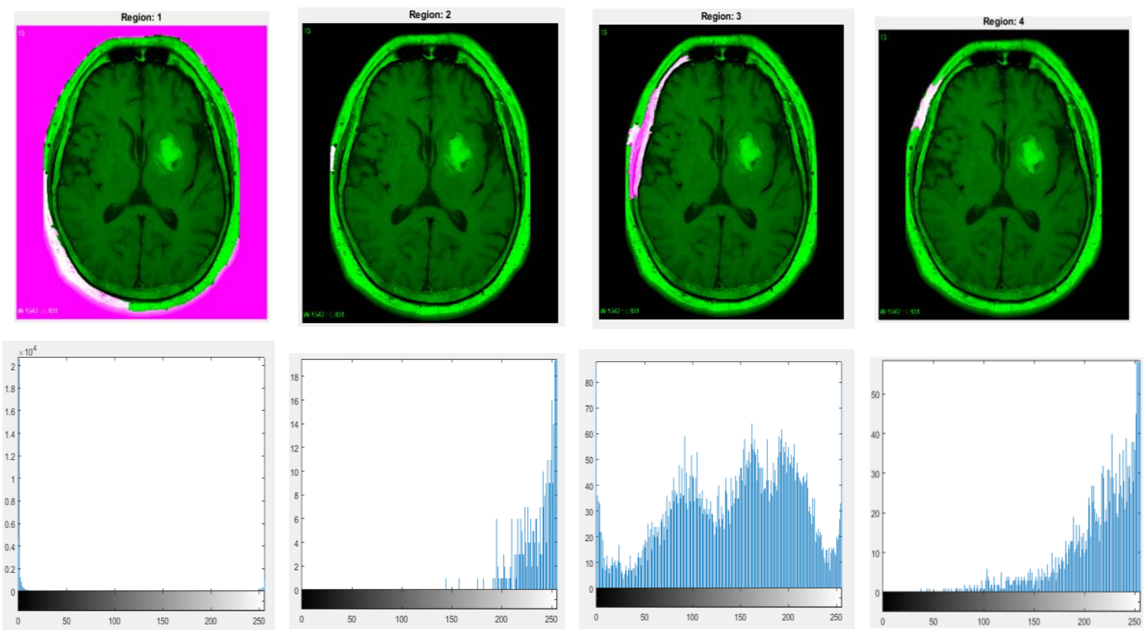

Figure 10 Histogram region

The next step performs region merging operation in the system first constructs zero matrices of the link map's size (Lm) (Step-5). The next process is to compute the estimation of overlapping factors between the two statistical samples. For this, the next process extracts the connected component of each segment (Step-6). Afterward, the system computes a histogram of the current point and connection point using cpt and cc. The overlapping factor (O_{vf}) is then computing using function f_s over the square root of both the current point and connecting point. The next process executes the operation of reconstruction using the value of overlapping factor divided by the sum of elements of both P and P1 using function f(x), and the computed result is further stored in cpt. This process of pre-classification is shown in Figure 11. Finally, a region merging is performed over C to compute the final classified and segmented region (Step-7).

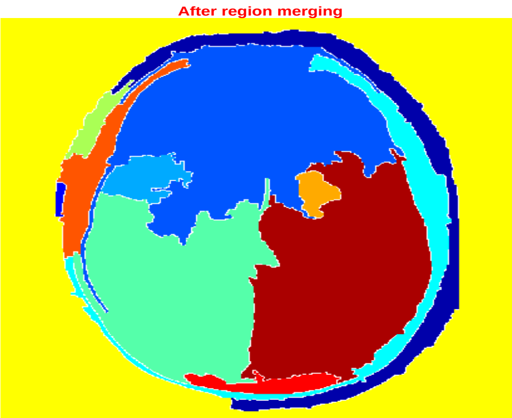

Figure 11 Pre classified image

Final Classification Process

This section describes the final stage of the proposed system, where it uses ANN for boosting the classification performance to detect tumors and their critical state. However, the ANN concept is because the system first selects to include correct input into the neurons before initiating the training process. To this end, the proposed system performs a feature extraction process in which all statistical values can be predicted. The system considers all standard descriptive statistical parameters on the MR brain image to estimate required features. Adopting ANN provides beneficial advantages in obtaining the inferences from vast amounts of data. Therefore, along with pattern extraction, significant trends can also be identified. Thus, the information obtained can be applied to develop information structures based on ANN. This newly constructed information includes an amount of extremely interconnected elements to deal with the classification problem. The training operation is performed by considering the previous operations, and also a real value function is considered to formulate activation function in ANN. Using this training method provides different benefits, such as predicting time series and function approximation. This training process includes a repetitive learning process until the system receives the finest classification information. Finally, after the training operation is completed, the proposed system can efficiently perform the classification of abnormalities from the MR image, whether there is a tumor or no tumor in the classified MR image. Therefore the next section demonstrates the computing steps for performing the final classification operation as follows:

Computing Steps for initiating Classification process

Step-1. Perform Feature Extraction
Step-2. Create an empty numeric matrix
   a. *Feature → [ ]*
   b. *Class → [ ]*
Step-3. For i = 1:fmax(β_{i2})
Step-4. Get region: R ← β_{i2} ==i
Step-5. Get region pixel value: R_{pv} ← I_m(R)
Step-6. Extract feature
   a. *F → f_{ext}(rpv)*
Step-7. Store values
   a. *Feature ← [feature F]*
Step-8. Perform ANN training
   a. *Load database*
   b. *Initialize variable for feature vector(Fv) and target vector (Tv)*
   c. *Compute all image detail*
Step-9. Perform the above procedures
   a. *Perform the first operation of the Image Processing Module (Section 5.3.1.1)*
   b. *Perform the Second operation of the Image Segmentation Process (Section 5.3.2.1)*
   c. *Perform the Second operation of initiating the Classification process (Section 5.3.3.1)*
   d. *Perform feature extraction operation(Section 5.3.4. 1 from Step-1 to Step-7)*
Step-10. Load Ground Truth (GT)
Step-11. Compute matching segment from GT
   a. *For i = 1:fmax(β_{i2})*
   b. *Get region: R ← β_{i2} ==i*
   c. *Extract Common regions: R_{comn} ← R(GT)*
   d. *Get R_{match} ← area of an object from R_{comn}*
   e. *End*
Step-12. Identified region: R_{id} → fmax(R_{match})
Step-13. Tumor Identified: T_{id} = β_{i2} ==i
Step-14. Save F_v and T_v
Step-15. Apply Neural Network
Step-16. Train radial basis ANN
   a. *Net → f_{radial} (F_v, T_v)*
Step-17. Perform ANN-based Classification
Step-18. Load ANN
Step-19. Class → Net (features)
Step-20. For For i = 1:fmax(β_{i2})
      a. *Get: ← R*
      i) ***Check:** (class(i)==2)*
         Flag → Malignant
         Otherwise:
            Flag benign
   End
Step21. Compute Accuracy TP, TN, FP, FN, Sensitivity, Specificity, Precision, and F1Score

Illustrations

Computing steps for initiating the final classification process begin with the feature extraction process, where all possible statistical characteristics are predicted (Step-1). In order to achieve this objective, the next step constructs an empty numeric matrix (Step-2). Further, the system again computes the region from the β_{i2} (second version of segmented image) computed in previous pre-classification operation also, the pixel value of the region is computed for obtaining detailed statistical characteristics for computing features (Step-3 to Step-5). The next process uses a feature extraction function over the region pixel value, stored into the empty numeric matrix (Step-7). The next process is executed for training operation by adding a Bayesian toolbox. After which the database loading process is performed with computing, all detail of image exists in the database. The assignment of a new variable for feature vector and target vector is carried for estimating a score for performing prediction based on the extracted feature (Step-8). The training process is performed by executing the previous computing steps implemented in the input image processing module, initial segmentation module, and the initial classification module (Step-9). The next steps perform the process of loading ground truth data from the given data sets subjected to extraction of matching segment and for computation of object present in the image (Step10 and Step-11). After this operation, maximum region matching is carried out from which a suspicious region is detected, and the tumor is identified (Step-12 and Step-13). The next process is to apply the ANN technique using function $f_{radial}(x)$ over the target vector and feature vector, which refers to the radial basis network (Step-16). A radial based network (Net) with the feature is assigned to a class variable initialized in the previous operation of feature extraction operation (Step-19). Based on the region class, the system performs a binary decision-making process for flagging whether the tumor in the brain is malignant or benign (Step-20). The next step computes the accuracy score in terms of multiple performance parameters. Figure 5.15 demonstrates the final result of the above-computed procedures for tumor classification from the brain MR image.

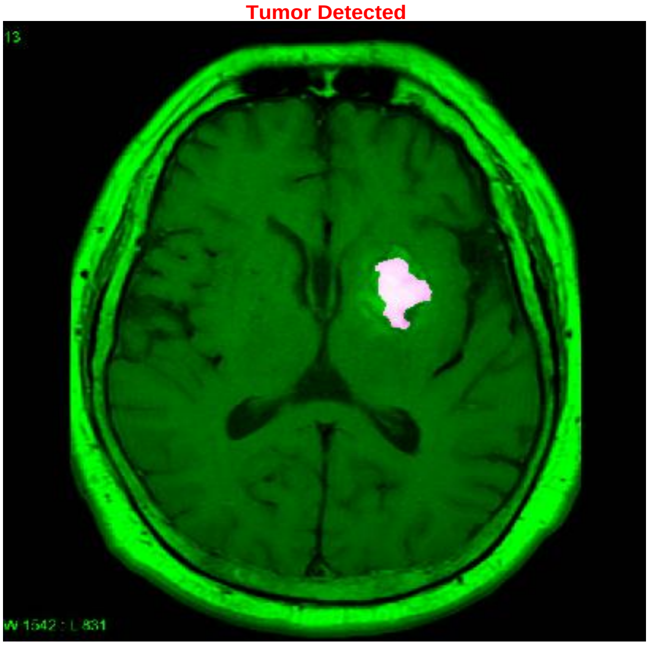

Figure 12 ANN-based tumor detection and classification

The above Figure 12 demonstrates the proposed HFC framework's outcome, which provides accurate tumor classification from the brain MR image.

Numerical Results

This section presents the numerical outcome of the proposed framework. However, the visual outcomes have already been presented in the above discussion of sequential operations. In order to assess the performances of the proposed work, a comparative analysis is made with the existing approaches of training such as SVM-support vector machine, feed-forward network. The proposed system subjects the implemented logic using a specific MATLAB method *svmtrain* which is used for training purpose and results associated all accuracy parameters (e.g. F1 score, precision, specificity, sensitivity, etc.) are obtained. Similarly, a MATLAB method known as *feedforwardnet* is used over the proposed logic of classification of brain tumor and similar accuracy parameters are obtained. All the numerical outcome of accuracy are stored in *.mat* file in MATLAB, from which plotting is carried out in order to obtain Figure 12. This assessment is carried out over complete brain MRI images in dataset and then the values of SVM and feedforward are averaged to obtained mean value of Existing system. The proposed system also considers a similar set of images for the comparative assessment to identify abnormal brain areas. The whole performance assessment is made in True Positive, True Negative, False Positive, False Negative, Sensitivity / Recall Rate, Specificity, Precision, and F1-Score.

Table-1 Comparative assessments in terms of abnormal regions in brain MRI

Accuracy Parameter	Proposed System	SVM Technique
F1-Score	0.647231	0.237852
Precision	0.48465	0.25446
Specificity	0.26553	0.49867
Sensitivity	0.89679	0.82741
False Negative	0.11574	0.29485
False Positive	0.76884	0.91748
True Negative	0.34891	0.49658
True Positive	0.89745	0.78945

The performance analysis demonstrated in Table.1 is performed considering the standard dataset. It can be observed from the outcome that the proposed system provides a valid accuracy value in terms of precision and F1-score values. The proposed system's overall computing time is 0.29671 seconds, while the existing system's computing time varies between 0.42883-1.6883 seconds. The proposed HFC system's performance accuracy is computed nearly to be 99%, and the proposed system provides significantly reduced false positives rate compared to existing training methods. The main reason behind this extensive classification process is that it provides a better feature extraction process. Therefore, it can be analyzed that the ANN tumor classification has a significant effect on the performance of the brain tumor classification from the MR image.

VI. CONCLUSION

The present study on brain tumours, demonstrates a promising approach to enhancing the accuracy and efficiency of brain tumor diagnosis. By leveraging histogram features extracted from MRI images, coupled with the predictive power of Artificial Neural Networks (ANN), this method provides a robust framework for classifying brain tumors. The use of histogram features allows for the capture of essential intensity patterns and variations within MRI images, which are crucial for distinguishing between different types of brain tumors. These features, when processed through an ANN, enable the model to learn complex patterns and relationships that are indicative of specific tumor classes. The ANN's ability to handle non-linearities and high-dimensional data makes it particularly well-suited for this task.

Our experimental results indicate that the proposed histogram-based approach, combined with ANN, achieves high classification accuracy, demonstrating its potential as a reliable tool for brain tumor classification. This method not only enhances diagnostic precision but also supports the rapid analysis of MRI scans, thereby aiding radiologists in making timely and informed decisions. Furthermore, the adaptability of ANNs allows for continuous improvement as more data becomes available, suggesting that the model can be refined and its performance enhanced over time. This scalability and flexibility are critical in clinical settings, where the diversity of tumor presentations requires adaptable and robust diagnostic tools.

In conclusion, the integration of histogram-based feature extraction with ANN presents a viable and effective strategy for brain tumor classification in MRI images. Future research could focus on refining feature selection methods, exploring deeper neural network architectures, and integrating multi-modal imaging data to further improve classification performance and clinical applicability. The findings from this study underscore the potential of advanced image processing techniques and machine learning in transforming medical diagnostics and improving patient outcomes.

References

1. *A. Jagan, "A New Approach for Segmentation and Detection of Brain Tumor in 3D Brain MR Imaging," 2018 Second International Conference on Electronics, Communication and Aerospace Technology (ICECA), Coimbatore, India, 2018, pp. 1230-1235, doi: 10.1109/ICECA.2018.8474874.*
2. *K. Pikulkaew, "Enhancing Brain Tumor Detection with Gradient-Weighted Class Activation Mapping and Deep Learning Techniques," 2023 20th International Joint Conference on Computer Science and Software Engineering (JCSSE), Phitsanulok, Thailand, 2023, pp. 339-344, doi: 10.1109/JCSSE58229.2023.10202020.*
3. *H. M. Moftah, N. I. Ghali, A. e. Hassanien and M. A. Ismail, "Volume identification and estimation of MRI brain tumor," 2012 12th International Conference on Hybrid Intelligent Systems (HIS), Pune, India, 2012, pp. 120-124, doi: 10.1109/HIS.2012.6421320.*
4. *W. Ahamad, V. Pal, Shreyash and M. K. Sharma, "Brain tumor detection using deep learning," 2023 5th International Conference on Advances in Computing, Communication Control and Networking (ICAC3N), Greater Noida, India, 2023, pp. 647-652, doi: 10.1109/ICAC3N60023.2023.10541811.*
5. *D. D. G, S. Doss, S. S and S. C. N, "Precision MRI Brain Tumor Identification: Leveraging Advanced Techniques for Accurate Classification," 2024 International Conference on Computing and Data Science (ICCDS), Chennai, India, 2024, pp. 1-5, doi: 10.1109/ICCDS60734.2024.10560447.*
6. *S. Alagarsamy, K. Kamatchi and V. Govindaraj, "A Novel Technique for identification of tumor region in MR Brain Image," 2019 3rd International conference on Electronics, Communication and Aerospace Technology (ICECA), Coimbatore, India, 2019, pp. 1061-1066, doi: 10.1109/ICECA.2019.8822188.*
7. *D. Patel, F. Vankawala and B. Bhatt, "A Survey on Identification of Glioblastoma Multiforme and Low-Grade Glioma Brain Tumor Type," 2019 International Conference on Communication and Signal Processing (ICCSP), Chennai, India, 2019, pp. 0335-0339, doi: 10.1109/ICCSP.2019.8698100.*
8. *Goswami and M. Dixit, "An Analysis of Image Segmentation Methods for Brain Tumour Detection on MRI Images," 2020 IEEE 9th International Conference on Communication Systems and Network Technologies (CSNT), Gwalior, India, 2020, pp. 318-322, doi: 10.1109/CSNT48778.2020.9115791.*
9. *Harish S B. H. Lavanya Vaishnavi D A and Anil Kumar C, "FILTER BASED ANALYSIS FOR THE MRI DATA IN BIOMEDICAL ENGINEERING", OGF, vol. 34, no. 3s, pp. 2476–2484, Jul. 2024.*
10. *R. Maurya and S. Wadhwani, "Morphology Based Brain Tumor Identification and Segmentation in MR Images," 2021 IEEE Bombay Section Signature Conference (IBSSC), Gwalior, India, 2021, pp. 1-6, doi: 10.1109/IBSSC53889.2021.9673338.*
11. *J. K. Periasamy, B. S and J. P, "Comparison of VGG-19 and RESNET-50 Algorithms in Brain Tumor Detection," 2023 IEEE 8th International Conference for Convergence in Technology (I2CT), Lonavla, India, 2023, pp. 1-5, doi: 10.1109/I2CT57861.2023.10126451.*
12. *C. Anil Kumar,1 S. Harish,1 Prabha Ravi,2 Murthy SVN,3 B. P. Pradeep Kumar, (2022) Lung Cancer Prediction from Text Datasets Using Machine Learning, Hindawi BioMed Research International Volume 2022, Article ID 6254177, 10 pages https://doi.org/10.1155/2022/6254177*
13. *S. D. Gupta, K. S. -e. Rabbani and Z. B. Mahbub, "Brain tumor identification through microstructure study using MRI," 2016 International Conference on Medical Engineering, Health Informatics and Technology (MediTec), Dhaka, Bangladesh, 2016, pp. 1-4, doi: 10.1109/MEDITEC.2016.7835395.*
14. *N. Kasabov, L. Zhou, M. Gholami Doborjeh, Z. Gholami Doborjeh and J. Yang, "New Algorithms for Encoding, Learning and Classification of fMRI Data in a Spiking Neural Network Architecture: A Case on Modeling and Understanding of Dynamic Cognitive Processes," in IEEE Transactions on Cognitive and Developmental Systems, vol. 9, no. 4, pp. 293-303, Dec. 2017.*
15. *R. Armañanzas, M. Iglesias, D. A. Morales and L. Alonso-Nanclares, "Voxel-Based Diagnosis of Alzheimer's Disease Using Classifier Ensembles," in IEEE Journal of Biomedical and Health Informatics, vol. 21, no. 3, pp. 778-784, May 2017.*
16. *J. Liu, M. Li, W. Lan, F. Wu, Y. Pan and J. Wang, "Classification of Alzheimer's Disease Using Whole Brain Hierarchical Network," in IEEE/ACM Transactions on Computational Biology and Bioinformatics, vol. 15, no. 2, pp. 624-632, 1 March-April 2018.*
17. *Harish S., Ali Ahammed G.F. (2019) Comprehensive Framework for Classification of Abnormalities in Brain MRI Using Neural Network. In: Silhavy R., Silhavy P., Prokopova Z. (eds) Computational Statistics and Mathematical Modeling*

Methods in Intelligent Systems. CoMeSySo 2019 2019. Advances in Intelligent Systems and Computing, vol 1047. Springer, Cham. https://doi.org/10.1007/978-3-030-31362-3_8

18. M. Liu, J. Zhang, E. Adeli and D. Shen, "Joint Classification and Regression via Deep Multi-Task Multi-Channel Learning for Alzheimer's Disease Diagnosis," in IEEE Transactions on Biomedical Engineering, vol. 66, no. 5, pp. 1195-1206, May 2019.

19. P. Kumar Mallick, S. H. Ryu, S. K. Satapathy, S. Mishra, G. N. Nguyen and P. Tiwari, "Brain MRI Image Classification for Cancer Detection Using Deep Wavelet Autoencoder-Based Deep Neural Network," in IEEE Access, vol. 7, pp. 46278-46287, 2019.

20. Y. Shao, J. Kim, Y. Gao, Q. Wang, W. Lin and D. Shen, "Hippocampal Segmentation From Longitudinal Infant Brain MR Images via Classification-Guided Boundary Regression," in IEEE Access, vol. 7, pp. 33728-33740, 2019.

21. L. Wang, C. Xie and N. Zeng, "RP-Net: A 3D Convolutional Neural Network for Brain Segmentation From Magnetic Resonance Imaging," in IEEE Access, vol. 7, pp. 39670-39679, 2019.

22. A. Gudigar, U. Raghavendra, E. J. Ciaccio, N. Arunkumar, E. Abdulhay and U. R. Acharya, "Automated Categorization of Multi-Class Brain Abnormalities Using Decomposition Techniques With MRI Images: A Comparative Study," in IEEE Access, vol. 7, pp. 28498-28509, 2019.

23. S. Harish & Ahammed, G.F. (2020). An optimized approach for extensive segmentation and classification of brain MRI. International Journal of Electrical and Computer Engineering (IJECE).